Alexandridis, T.K., Sotiropoulou, A.M., Bilas, G., Karapetsas, N., and Silleos, N.G., 2014. The effects of seasonality in estimating the C-factor of soil erosion studies. Land Degradation and Development, DOI: 10.1002/ldr.2223.

THE EFFECTS OF SEASONALITY IN ESTIMATING THE C-FACTOR OF SOIL EROSION STUDIES

Short title: Effects of seasonality in estimating the C-factor

THOMAS K. ALEXANDRIDIS[1*], ANASTASIA M. SOTIROPOULOU[1], GEORGE BILAS[2], NIKOLAOS KARAPETSAS[1], NIKOLAOS G. SILLEOS[1]
[1] Lab of Remote Sensing and GIS, School of Agriculture, Aristotle University of Thessaloniki, Thessaloniki 54124, Greece
[2] Lab of Applied Soil Science, School of Agriculture, Aristotle University of Thessaloniki, Thessaloniki 54124, Greece

[*] Corresponding author
Thomas Alexandridis (thalex@agro.auth.gr)
Address: Lab of Remote Sensing and GIS, School of Agriculture, Aristotle University of Thessaloniki, University Campus, University Box 259, 54124 Thessaloniki, Greece
Tel: +302310 991757, Fax: +302310 991778

ABSTRACT

Monitoring soil erosion risk is an important part of soil conservation practices. It is usually estimated with the Universal Soil Loss Equation, and the C-factor (vegetation cover) is derived from optical satellite images. However, due to lack of data and resources, or in rapid assessments, C-factor is estimated using one or a few satellite observations, despite being temporally variable according to plants' phenology. The aim of this work was to study the effect of seasonality in estimating C-factor. This was achieved by demonstrating first that there is a difference when estimating soil erosion with USLE at variable time steps in a year, namely once, seasonally and monthly. Using MODIS NDVI images and statistical analysis at subcatchment scale, it was shown that there is a significant difference when estimating mean annual soil loss with the above mentioned temporal options. The highest differences were observed between monthly and annual time steps. The second objective was to identify which is the optimum time to estimate C-factor in a year. The results show that November, October or March are the optimum months for single image estimation of annual soil erosion. Statistical analysis with a random point dataset suggested that the spatial variability of the results was influenced by the land cover type, especially in areas with variable leaf cover where a single date estimation of C-factor was not representative of the whole year, such as annual crops and deciduous trees.

Keywords: soil erosion, USLE, seasonality, remote sensing, GIS

INTRODUCTION

Soil erosion is probably the most dangerous form of soil degradation worldwide, which is caused by both natural and human factors. More specifically, for the Mediterranean ring, scenarios of climate change indicate high and increasing erosion risk, due to sparse vegetation, low soil structural stability, non-negligible slopes, and intense rainstorms (Cheviron *et al*., 2011). Land cover changes, often due to forest

fires, intensive grazing, and changes of agricultural patterns, have also been contributing to Mediterranean land degradation (Cerdà *et al.*, 2010). Knowledge of rates of soil erosion by water is important for three principal reasons. First, it is essential to our understanding of landform development. Secondly, on agricultural land, these rates determine the long-term sustainability of agricultural practices and have profound economic consequences (Doran, 2002, Pimentel *et al.*, 1995). Finally, the eroded material provides the source of organic and inorganic materials which are transported to downstream water bodies thus accelerating sedimentation and impacts on water quality (Nezlin *et al*., 2005).

Monitoring soil erosion in-situ is very costly and usually limited to small experimental sites. Thus, several approaches to soil erosion modeling have been developed: physical models (e.g. PESERA), conceptual models (e.g. SWIM) and empirical models (e.g. USLE) (Kirkby *et al.*, 2008, Krysanova *et al.*, 1998, Wischmeier & Smith, 1978). All models, be they simple black box or complex, process-based structures, require parameters that are often troublesome to estimate accurately. Input parameters are difficult to estimate with any degree of precision because of the limitations of available measurement techniques and spatial and temporal variability (Brazier *et al*., 2000). The most widely applied empirical erosion model is the Universal Soil Loss Equation (USLE) which was developed especially to calculate soil erosion rates in agricultural areas as a function of soil erodibility, topography, rainfall, management and cover factors (Wischmeier & Smith, 1978). After USLE, several other improvements have been proposed (RUSLE, MUSLE, and others) which are based on the basic empirical approach (Renard *et al.*, 1991, Williams, 1975). Nevertheless, USLE remains the most widely used model for soil erosion (Kinnell, 2010).

Finding data at the appropriate spatial and temporal scales to feed into soil erosion models has been a major problem in their application. Geographic Information Systems (GIS) and remote sensing are powerful tools for investigating the status of natural resources (Morain, 1998). Capitalizing on the advantages of remote sensing as a source of data and the spatial analysis capabilities of GIS, several adaptations of soil erosion models have been presented. These have been applied from the farm level to regional extents, from 0.6m to 1100m spatial resolution, and from monthly to annual time steps (Symeonakis & Drake, 2004, Thiam, 2003, Vrieling, 2006).

Specifically for USLE, the soil erodibility (K) and topography (LS) factors are constant over long periods, and their spatial scale has only troubled the researchers (Angulo-Martínez *et al.*, 2009, Panagos *et al.*, 2012). The rainfall factor (R) is seasonally variable and meteorological stations routinely collect data which are available at low cost. Models and satellite images have been used to increase the spatial distribution of R (Meusburger *et al.*, 2012, Zhu *et al.*, 2011). The vegetation cover factor (C) is also seasonally variable, however its estimation requires acquisition of satellite images and digital image processing work. This is the main reason why C-factor is usually estimated using a single satellite image (de Asis & Omasa, 2007, Ismail & Ravichandran, 2008) or only a few (Folly *et al*., 1996). In these studies the selection of the time of image acquisition is arbitrary and unjustified, although it may considerably influence the resulting soil erosion estimate (Hessel, 2005, Vrieling, 2006).

The aim of this work is to study the effect of seasonality in estimating the C-factor of USLE. The specific objectives include: (i) to demonstrate that there is a difference when estimating soil erosion with USLE at variable time steps in a year, and (ii) to identify which is the optimum time to estimate C-factor in a year. The results were examined together with the land cover and other factors that influence the seasonality of soil erosion.

MATERIALS AND METHODS

Study area

The study area consists of the 10 main river basins of north Greece, including their extension to adjacent countries in cases of transboundary rivers (Figure 1). The total area is 119,000 km^2 and is subdivided in 65 subcatchments (Strahler level 5) to facilitate analysis. Small coastal basins (less than 1,500 km^2) were excluded from analysis. A large sub-basin of Evros/Maritsa falling in European Turkey was also excluded due to lack of soil and land cover data.

The southern part of the study area is characterized by the Mediterranean climate, while the northern inland part is continental. Annual rainfall ranges from about 400mm in the lowland coastal areas to more than 1500mm in the mountain regions (Tockner *et al*., 2008). Elevation ranges from 0 to 2925 m.a.s.l. and mountains cover the largest part of the study area, forming alluvial valleys. The land use is mainly arable land in the lowland valleys and natural vegetation in higher elevations (43% and 53% respectively, according to CLC2000). Soil textural class (according to the European Soil Database) is characterized as medium in the central and south part, medium fine to fine in the northeast part, and coarse in the northwest part.

According to UNCCD (United Nations Convention to Combat Desertification), the area is prone to desertification due to the particular conditions, which include poor and highly erodible soils, and uneven distribution of rainfall.

Datasets and processing

The soil erosion risk was estimated by the USLE. As seen in the description of each factor, data from remote sensing were utilized as much as possible.

$$A = C\ R\ K\ LS\ P$$

where:

- A is the estimated annual soil loss in Mg ha^{-1} y^{-1}.
- C is the cover factor (unitless). It is defined as the ratio of soil loss under the given vegetation cover to that which would occur under continuously bare soil. This was estimated from the equation: C = exp (-a (NDVI / (b - NDVI))), where NDVI is the Normalized Difference Vegetation Index, and a and b are constants derived from a similar work in Italy (Van der Knijff *et al*., 1999). The NDVI images were acquired by the MODIS sensor (Moderate Resolution Imaging Spectroradiometer) on board the Terra satellite. To avoid data gaps because of frequent cloud cover during the rainy season, the product

MOD13Q1 "Vegetation Indices" was used, which is a 16-day composite at 250 m spatial resolution that is available globally (https://lpdaac.usgs.gov/products/modis_products_table/mod13q1). The data were downloaded from NASA (https://wist.echo.nasa.gov/) at a monthly time step.

- R is the rainfall erodibility factor (MJ mm ha^{-1} hr^{-1} yr^{-1}) which represents the driving force for rain erosion. It takes into consideration the total rainfall and, more important, the intensity and seasonal distribution of the rain. It was approximated using the Modified Fournier Index (Arnoldus, 1978): $MFI=\Sigma(p_i^2 / p)$, where p_i is the mean monthly rainfall (mm) and p is the mean annual rainfall (mm). The cumulative precipitation volume was estimated from TRMM (Tropical Rainfall Mapping Mission) data (http://trmm.gsfc.nasa.gov/), using the product "3B43" (mean monthly rainfall) at 0.25^o spatial resolution. TRMM uses a precipitation radar, a passive microwave imager and a visible and infrared scanner to estimate precipitation volumes at high spatial and temporal resolutions.
- K is the soil erodibility factor (Mg ha hr ha^{-1} MJ^{-1} mm^{-1}). This was estimated from the European Soil Database (Panagos, 2006) at a scale 1:1,000,000 (Van der Knijff *et al*., 2000).
- L, S: the topographic factors (unitless) account for the effects of slope steepness and slope length on erosion. These were calculated from the equation described in Moore and Burch (1986): $LS = (A_f C / 22.13)^{0.4} (\sin\beta / 0.0896)^{1.3}$, where A_f is the flow accumulation (pixels), C is the pixel size (m), and β is the slope angle. A digital elevation model from SRTM (Shuttle Radar Topography Mission) data at 90 m spatial resolution (http://srtm.usgs.gov/) was used to estimate the flow accumulation and slope.
- P: supporting practices. In absence of data, this was set to 1.

Additional datasets used were:

- CLC2000: The CORINE Land Cover of year 2000 (EEA, 2004), with minimum mapping unit of 25 ha, which was the most recent available for the entire study area.
- Subcatchments from the "European Catchment Characterisation and Modelling" project (Vogt *et al*., 2007).

The temporal frame of analysis included two hydrological years from July 2009 to June 2011.

Formulation of objective functions and statistical analysis

The first objective of this work was to demonstrate that there is a difference when estimating the C-factor with variable time steps. Thus, the annual soil loss was estimated with the C-factor derived from three options: (i) once "A1", i.e. using 1 satellite image per year, (ii) seasonally "A4", i.e. using 4 satellite images per year, and (iii) monthly "A12", i.e. using 12 satellite images. Considerable variations among the three options would suggest an effect of seasonality in C-factor estimation.

In support of previous work that had used a single date C-factor estimation, the second objective is to identify the optimum single date NDVI image that can be used to provide a good estimate of the annual soil loss. Thus, the estimated soil loss of each month was compared with the mean monthly, and the month with the lowest difference was selected as the optimum single time to estimate C-factor. This is based on the assumption that the best estimate of C is when using many satellite images which are each representative of a short period.

Analysis was carried out at the subcatchment level, i.e. the mean soil loss and other factors were calculated for each of the 65 subcatchments. Furthermore, a sample of 10000 randomly selected points was used for statistical analysis. This was done to reveal patterns and interactions (e.g. with land cover type) which was not possible at the subcatchment level. However, the subcatchment level was used to facilitate the presentation and interpretation of the results.

Repeated analysis of variance (ANOVA), logistic regression and contingency analysis were used to test for the effects of land cover type, year, rainfall, slope, and annual soil loss, and their interactions on the resulting differences and optimum month. F-tests and Chi-tests from these analyses were used to test the main effects and interactions. These analyses allowed a more detailed observation of interactions as compared to the subcatchment means.

RESULTS AND DISCUSSION

Differences in soil erosion estimate because of seasonality

The average estimated annual soil loss was calculated per subcatchment and results were compared among the three options ("A1", "A4" and "A12") using paired T-test. Table 1 presents the resulting annual soil loss (aggregated per river basin) and the differences across the three options.

Results suggest that there is a consistent significant overestimation of annual soil loss with option A1 as compared with A12, with a mean difference of 9.37 Mg ha^{-1} y^{-1}. This was expected because of the selection of the single image in November, a time when most annual crops have been harvested and most of the deciduous trees have dropped their leaves, thus leaving very sparse or no vegetation cover.

With option A4, soil loss is again overestimated as compared to A12. Although significantly different, the mean difference of 4.55 Mg ha^{-1} y^{-1} is lower than the one observed between options A1 and A12. This is due to the better approximation of the seasonal phenologic changes of natural and agricultural vegetation.

Further point analysis was employed to investigate the effects of various parameters on the results (Table 2). The overestimation of annual soil loss is consistently higher in areas covered by natural vegetation (mean = 11.71 Mg ha^{-1} y^{-1}), as compared to the agricultural areas (mean = 3.92 Mg ha^{-1} y^{-1}). More specific, analysis of variance of the differences by CLC2000 land cover type, shows "sparsely vegetated areas", "broad-leaved forest" and "natural grassland" having the highest differences across the three options, as compared to "coniferous forest" and "schlerophylous vegetation". "Agricultural land covered by complex cultivation patterns", "olive groves",

"vineyards" and "non-irrigated arable land" show the highest differences across the three options, as compared to "permanently irrigated land" and "rice fields". This could be mainly due to the variation of canopy cover across the year, which provides a high level of inaccuracy when soil loss is estimated infrequently (annually or seasonally). Finally, the results are consistent across the two years, with the mean difference 0.83 Mg ha^{-1} y^{-1} (F=3.623, DF=388, P=0.058).

The spatial distribution of the differences in estimating annual soil loss between the three options is displayed in Figures 2 and 3. All subcatchments show a positive difference across the three options, in the same way as the river basin level. There are several subcatchments that display a very high difference across the three options. These are located at the upstream and mountainous areas of Aliakmon, Strimon/Struma and Nestos/Mesta river basins. According to the ANOVA, it seems that land cover is influencing this behaviour, as the main land cover type is herbaceous or deciduous natural vegetation. In contrast, the lowest differences are displayed in the cultivated plains of Axios/Vardar and Evros/Maritsa river basins.

Optimum time to estimate C-factor

The frequency distribution of the optimum month to estimate C-factor for both years is displayed in Figure 4 and their spatial distribution in Figure 5.

November is most frequently the optimum month for estimating annual soil loss, followed closely by March and October. This could be due to the low vegetation coverage during these wet months, which renders them high in the rank of erosion risk. It is worth noting that the dry, fully covered by vegetation months of May to August were not optimum for the estimation of annual soil loss for any of the subcatchments.

In Figure 5 there is a tendency for March and October as the optimum month at the cultivated plains of the river basins, while November, December and January are more frequently the optimum months at the upstream and mountainous areas. This could be the effect of the variability of rain and land cover distribution within each heterogeneous subcatchment.

Further analysis was employed to investigate the effects of various parameters on the results. Contingency analysis of the distribution of the optimum month per land cover type has shown a pattern related to major land cover type (Table 3). More specifically, there is a tendency for the autumn months to be the optimum ones in the agricultural land, while March is optimum more frequently in the natural vegetation. This could be due to the soil preparatory cultivation processes which usually occur in October, leaving the soil exposed to rain erosion. On the contrary, the areas with natural vegetation are covered by canopy to a variable degree throughout the year (e.g. grass or bush covers the soil even when the leaves in a deciduous forest have dropped), thus the preference for March may be influenced by the high rainfalls of spring.

Logistic regression has revealed that other parameters which might have an influence on the selection of the optimum month (mean annual rainfall, slope, and annual soil erosion), in fact have no effect (Table 4). Furthermore, contingency analysis with Chi-square statistic was used to confirm that the distribution of the optimum month is the

same across the examined years (N = 130, Pearson's Chi-square = 11.703, P = 0.3054).

Discussion and implications for land management

This research contributes to the more accurate and easy estimation of soil erosion. A GIS model has been selected where all input data (except soil erodibility) have been estimated from remote sensing. The results have identified cases where a single satellite image or a few images per year can provide an acceptable estimate of C-factor and thus of soil erosion. This is important in locations with limited data availability or for rapid assessment of large areas, similar to programs of the FAO in Africa (FAO, 1983).

Regarding the first objective, LULC seems to explain the results, i.e. the type of land cover influences the possibility that annual soil loss can be estimated equally by one, four or twelve satellite observations of C-factor in a year. As expected, the differences between the three options were higher in areas with vegetation of variable leaf cover such as annual crops and deciduous trees. The latter category showed, in fact, the highest differences because of the combined effect of rain-slope-cover, as deciduous trees are located on the highest slopes that also receive the highest rainfall when they have lost their leaves and before the spring leaf-out. Other studies in the Mediterranean have found similar patterns of soil loss according to rain distribution and land cover type (De Jong *et al.*, 1999, Diodato & Bellocchi, 2007, Kosmas *et al.*, 1997, Panagos *et al.*, 2011). In addition to the direct erosive capacity of rainfall, soil hydrology is an important factor influencing the seasonal variations of soil erosion through the change of infiltration rate (Cerdà, 1996, Cerdà, 1997).

Regarding the second objective, the temporal distribution of soil loss in the annual cycle and the high seasonal differences are the major factors that control the selection of the optimum month. It seems that November and March, the months most frequently appearing as the optimum ones for single observation of soil loss estimation, have a combination of high rainfall erosivity (R-factor) and low vegetation cover (high C-factor). The other months have considerably lower erosion risk, thus their selection as optimum would have led to the severe underestimation of annual soil loss. Equivalent results have been reported in another study that involved the identification of erosion features in grasslands (Vrieling *et al*., 2008), where it was concluded that the assessment of soil erosion with a single satellite image can be successful if it represents the vegetation cover during the time of the major erosion events.

Soil erosion shows a high level of spatial variability, as the parameters that influence it show an equally high spatial heterogeneity (Nearing *et al*., 1999). In this work, aggregated statistics per sub-catchment have been used to draw some of the results, whose representativity can be questionable in highly variable environments (Alexandridis *et al*., 2010). For this reason, randomly sampled point analysis was preferred, and aggregated statistics were used mainly for presentation purposes.

It should be clarified that at these scales, USLE estimates the soil erosion risk rather than actual soil loss, which is very costly and can only be measured at plot scale. The reported accuracy of USLE is variable but acceptable in similar studies around the

study area (Kosmas *et al.*, 1997, Panagos *et al.*, 2011). Another source of uncertainty in this work is the selected spatial and temporal scale. The pixel size of 250m for describing C (the main focus of this study) may seem large, however it has been proven adequate for regional studies of vegetation monitoring (Alexandridis *et al.*, 2008, Ferreira & Huete, 2004). Also, detailed weather data are needed in erosion studies in order to capture even a single rain event that could be very grave (Edwards & Owens, 1991). The selected monthly time step is similar to the one used in previous work performed around the study area (Panagos *et al*., 2011) and in other Mediterranean sites (Diodato, 2005).

The outcomes of this work could be useful for projects related to the Soil Protection Strategy of the EU. For instance, the low cost flow of information would be invaluable to help coordinate soil conservation actions aimed at combating soil degradation (Grimm *et al*., 2002). Policy makers could be provided with lower cost or more frequently available information to support their strategies. They could focus on distributing land management practices per month and per region in order to minimize the soil erosion risk. Furthermore, the results could easily feed into a soil observatory in order to be disseminated more easily and help create awareness. At the local level, this work could provide fast and low cost information that would help inform farmers and agronomists regarding the soil erosion risk through a web information system.

CONCLUSIONS

There is a significant difference in the estimation of soil loss by erosion when using variable time steps (expressed as 1, 4 or 12 images) for the C factor. The optimum months for single date estimation of annual soil loss are November, October, or March. The main factor that controls the spatial distribution of the results is the type of vegetation cover, specifically the variability of winter foliage loss.

ACKNOWLEDGEMENTS

MODIS and TRMM data were obtained through the online Data Pool at the NASA Land Processes Distributed Active Archive Center (LP DAAC) and Goddard Space Flight Center (GSFC). Authors are grateful to the anonymous reviewers for their constructive comments.

REFERENCES

Alexandridis TK, Gitas IZ, Silleos NG. 2008. An estimation of the optimum temporal resolution for monitoring vegetation condition on a nationwide scale using MODIS/Terra data. *International Journal of Remote Sensing* **29**:3589-3607.

Alexandridis TK, Katagis T, Gitas IZ, Silleos NG, Eskridge KM, Gritzas G. 2010. Investigation of aggregation effects in vegetation condition monitoring at a national scale. *International Journal of Geographical Information Science* **24**:507-521.

Angulo-Martínez M, López-Vicente M, Vicente-Serrano SM, Begueria S. 2009. Mapping rainfall erosivity at a regional scale: A comparison of interpolation methods in the Ebro Basin (NE Spain). *Hydrology and Earth System Sciences* **13**:1907-1920.

Arnoldus HMJ. 1978. An approximation of the rainfall factor in the universal soil loss equation, p. 127-132, *In* M. De Boodt and D. Gabriels, eds. *Assessment of Erosion*. John Wiley and Sons, Chichester, Great Britain.

Brazier RE, Beven KJ, Freer J, Rowan JS. 2000. Equifinality and uncertainty in physically based soil erosion models: Application of the glue methodology to wepp-the water erosion prediction project-for sites in the UK and USA. *Earth Surface Processes and Landforms* **25**:825-845.

Cerdà A. 1996. Seasonal variability of infiltration rates under contrasting slope conditions in southeast Spain. *Geoderma* **69**:217-232.

Cerdà A. 1997. Seasonal changes of the infiltration rates in a mediterranean scrubland on limestone. *Journal of Hydrology* **198**:209-225.

Cerdà A, Lavee H, Romero-Diaz A, Hooke J, Montanarella L. 2010. Preface: Soil erosion and degradation in Mediterranean type ecosystems. *Land Degradation and Development* **21**:71-74.Cheviron B, Le Bissonnais Y, Desprats JF, Couturier A, Gumiere SJ, Cerdan O, Darboux F, Raclot D. 2011. Comparative sensitivity analysis of four distributed erosion models. *Water Resources Research* **47**.

de Asis AM, Omasa K. 2007. Estimation of vegetation parameter for modeling soil erosion using linear Spectral Mixture Analysis of Landsat ETM data. *ISPRS Journal of Photogrammetry and Remote Sensing* **62**:309-324.

De Jong SM, Paracchini ML, Bertolo F, Folving S, Megier J, De Roo APJ. 1999. Regional assessment of soil erosion using the distributed model SEMMED and remotely sensed data. *Catena* **37**:291-308.

Diodato N. 2005. Predicting RUSLE (Revised Universal Soil Loss Equation) monthly erosivity index from readily available rainfall data in Mediterranean area. *Environmentalist* **26**:63-70.

Diodato N, Bellocchi G. 2007. Estimating monthly (R)USLE climate input in a Mediterranean region using limited data. *Journal of Hydrology* **345**:224-236.

Doran JW. 2002. Soil health and global sustainability: Translating science into practice. *Agriculture, Ecosystems and Environment* **88**:119-127.

Edwards WM, Owens LB. 1991. Large storm effects on total soil erosion. *Journal of Soil & Water Conservation* **46**:75-78.

EEA. 2004. CORINE Land Cover 2000 map [Online]. Available by European Environment Agency http://dataservice.eea.europa.eu/dataservice/ (verified 29/11/2005).

FAO. 1983. Keeping the land alive. FAO Soils bulletin 50, Soil erosion - its causes and cures. Food and Agriculture Organization of the United Nations, Rome.

Ferreira LG, Huete AR. 2004. Assessing the seasonal dynamics of the Brazilian Cerrado vegetation through the use of spectral vegetation indices. *International Journal of Remote Sensing* **25**:1837-1860.

Folly A, Bronsveld MC, Clavaux M. 1996. A knowledge-based approach for C-factor mapping in Spain using Landsat TM and GIS. *International Journal of Remote Sensing* **17**:2401-2415.

Grimm M, Jones R, Montanarella L. 2002. Soil Erosion Risk in Europe. European Soil Bureau, Institute for Environment & Sustainability, JRC Ispra.

Hessel R. 2005. Effects of grid cell size and time step length on simulation results of the Limburg soil erosion model (LISEM). *Hydrological Processes* **19**:3037-3049.

Ismail J, Ravichandran S. 2008. RUSLE2 model application for soil erosion assessment using remote sensing and GIS. *Water Resources Management* **22**:83-102.

Kinnell PIA. 2010. Event soil loss, runoff and the Universal Soil Loss Equation family of models: A review. *Journal of Hydrology* **385**:384-397.

Kirkby MJ, Irvine BJ, Jones RJA, Govers G, Boer M, Cerdan O, Daroussin J, Gobin A, Grimm M, Le Bissonnais Y, Kosmas C, Mantel S, Puigdefabregas J, Van Lynden G. 2008. The PESERA coarse scale erosion model for Europe. I. - Model rationale and implementation. *European Journal of Soil Science* **59**:1293-1306.

Kosmas C, Danalatos N, Cammeraat LH, Chabart M, Diamantopoulos J, Farand R, Gutierrez L, Jacob A, Marques H, Martinez-Fernandez J, Mizara A, Moustakas N, Nicolau JM, Oliveros C, Pinna G, Puddu R, Puigdefabregas J, Roxo M, Simao A, Stamou G, Tomasi N, Usai D, Vacca A. 1997. The effect of land use on runoff and soil erosion rates under Mediterranean conditions. *Catena* **29**:45-59.

Krysanova V, Müller-Wohlfeil DI, Becker A. 1998. Development and test of a spatially distributed hydrological/water quality model for mesoscale watersheds. *Ecological Modelling* **106**:261-289.

Meusburger K, Steel A, Panagos P, Montanarella L, Alewell C. 2012. Spatial and temporal variability of rainfall erosivity factor for Switzerland. *Hydrology and Earth System Sciences* **16**:167-177.

Moore ID, Burch GJ. 1986. Physical basis of the length-slope factor in the universal soil loss equation. *Soil Science Society of America Journal* **50**:1294-1298.

Morain SA. 1998. *GIS solutions in natural resource management* OnWord Press, Santa Fe, N.M.

Nearing MA, Govers G, Norton LD. 1999. Variability in soil erosion data from replicated plots. *Soil Science Society of America Journal* **63**:1829-1835.

Nezlin NP, DiGiacomo PM, Stein ED, Ackerman D. 2005. Stormwater runoff plumes observed by SeaWiFS radiometer in the Southern California Bight. *Remote Sensing of Environment* **98**:494-510.

Panagos P. 2006. The European soil database. *GEO: connexion* **5**:32-33.

Panagos P, Karydas CG, Gitas IZ, Montanarella L. 2011. Monthly soil erosion monitoring based on remotely sensed biophysical parameters: a case study in Strymonas river basin towards a functional pan-European service. *International Journal of Digital Earth* **5**:461-487.

Panagos P, Meusburger K, Alewell C, Montanarella L. 2012. Soil erodibility estimation using LUCAS point survey data of Europe. *Environmental Modelling and Software* **30**:143-145.

Pimentel D, Harvey C, Resosudarmo P, Sinclair K, Kurz D, McNair M, Crist S, Shpritz L, Fitton L, Saffouri R, Blair R. 1995. Environmental and economic costs of soil erosion and conservation benefits. *Science* **267**:1117-1122.

Renard KG, Foster GR, Weesies GA, Porter JP. 1991. Revised universal soil loss equation. *Journal of Soil and Water Conservation* **46**:30-33.

Symeonakis E, Drake N. 2004. Monitoring desertification and land degradation over sub-Saharan Africa. *International Journal of Remote Sensing* **25**:573-592.

Thiam AK. 2003. The causes and spatial pattern of land degradation risk in southern Mauritania using multitemporal AVHRR-NDVI imagery and field data. *Land Degradation and Development* **14**:133-142.

Tockner K, Robinson CT, Uehlinger U. 2008. *Rivers of Europe* Academic Press, London.

Van der Knijff JM, Jones RJA, Montanarella L. 1999. Soil erosion risk assessment in Italy. EUR 19022 EN., pp. 54. European Soil Bureau. Joint Research Center of the European Commission.

Van der Knijff JM, Jones RJA, Montanarella L. 2000. Soil erosion risk assessment in Europe. EUR 19044 EN., pp. 34. European Soil Bureau. Joint Research Center of the European Commission.

Vogt J, Soille P, de Jager A, Rimaviciute E, Mehl W, Foisneau S, Bodis K, Dusart J, Paracchini ML, Haastrup P, Bamps C. 2007. A pan-European River and Catchment Database. EC-JRC (Report EUR 22920 EN), pp. 120, Luxembourg.

Vrieling A. 2006. Satellite remote sensing for water erosion assessment: A review. *Catena* **65**:2-18.

Vrieling A, de Jong SM, Sterk G, Rodrigues SC. 2008. Timing of erosion and satellite data: A multi-resolution approach to soil erosion risk mapping. *International Journal of Applied Earth Observation and Geoinformation* **10**:267-281.

Williams JR. 1975. Sediment-yield prediction with Universal Equation using runoff energy factor. Present and Prospective Technology for Predicting Sediment Yields and Sources, ARS-S-40, pp. 244-252. US Department of Agriculture, Agricultural Research Service.

Wischmeier WH, Smith DD. 1978. Predicting rainfall erosion losses - A guide for conservation planning, pp. 537. U.S. Department of Agriculture, Agriculture Handbook.

Zhu Q, Chen X, Fan Q, Jin H, Li J. 2011. A new procedure to estimate the rainfall erosivity factor based on Tropical Rainfall Measuring Mission (TRMM) data. *Science China Technological Sciences* **54**:2437-2445.

Tables

Table 1: Estimated annual soil loss (A, in Mg ha^{-1} y^{-1}) aggregated per river basin using (a) A1 - one satellite image, (b) A4 - four satellite images, and (c) A12 - twelve satellite images

River basin	A1	A4	A12
Evros/Maritsa	15.68	13.14	10.65
Axios/Vardar	27.65	23.87	19.94
Strimon/Struma	27.85	23.08	18.24
Nestos/Mesta	33.70	28.03	20.56
Loudias	22.34	20.71	15.00
Aliakmon	41.06	33.06	28.82
Lissos	22.94	17.31	11.90
Vistonida	35.19	25.31	16.50
Gallikos	8.20	6.64	4.39
Mygdonia	7.66	7.59	4.37
Differences at the subcatchment level	A1 - A12 = 9.37** (N=130, t=6.138, P < 0.0001)		
	A4 - A12 = 4.55** (N=130, t=8.134, P < 0.0001)		
	A1 - A4 = 4.81** (N=130, t=4.431, P < 0.0001)		

** Denotes statistical significance at the 99% level

Table 2: Analysis of variance and effect of various parameters on the differences across the options of estimating annual soil loss (point analysis, N = 16608)

Effect	Class means (Mg ha^{-1} y^{-1})	P
Main LC on Differences		<0.001**
"natural"	11.71	
"agricultural"	3.92	
CLC type on Differences		<0.001**
"sparsely vegetated areas"	35.92	
"broad-leaved forest"	18.24	
"natural grassland"	13.77	
"coniferous forest"	7.00	
"schlerophylous vegetation"	11.56	
"complex cultivation patterns"	5.94	
"olive groves"	5.22	
"vineyards"	5.16	
"non-irrigated arable land"	4.26	
"permanently irrigated land"	0.61	
"rice fields"	0.92	
Year on Differences		0.058
2009	2.83	
2010	3.66	

** Denotes statistical significance at the 99% level

Table 3: Contingency analysis for the effect of CLC type on the selection of a single optimum month for estimating annual soil loss (point analysis, N = 16608)

CLC land cover type	**Optimum month**	**Frequency of appearance (%)**
Non-irrigated arable land	September	16.79
Permanently irrigated land	October	15.35
Rice fields	December	22.58
Vineyards	October	18.52
Fruit trees and berry plantations	November	21.38
Olive groves	December	33.33
Pastures	March	16.14
Complex cultivation patterns	November	17.26
Principally agricultural, with significant areas of natural vegetation	March	21.66
Broad-leaved forest	March	33.5
Coniferous forest	March	23.06
Mixed forest	March	28
Natural grasslands	March	25.63
Moors and heathland	January	37.66
Sclerophyllous vegetation	March	29.42
Transitional woodland-shrub	March	32.29
Pearson's Chi-square = 4212.8, P<0.001**		

** Denotes statistical significance at the 99% level

Table 4: Logistic regression analysis for the effect of various parameters on the selection of a single optimum month for estimating annual soil loss (at subcatchment level, N=130)

Effect	**Chi-square**	**P**
Mean annual rainfall	10.14	0.1810
Slope	8.52	0.2887
Annual soil erosion	9.72	0.2052

Figures

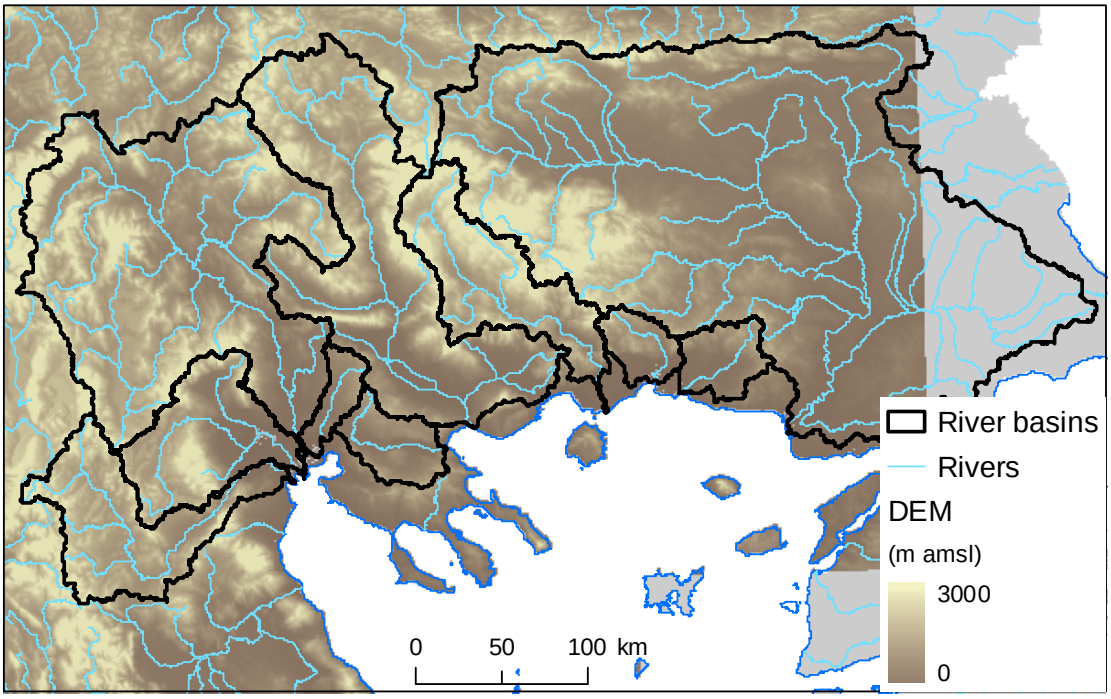

Figure 1: River basins and topography in the study area.

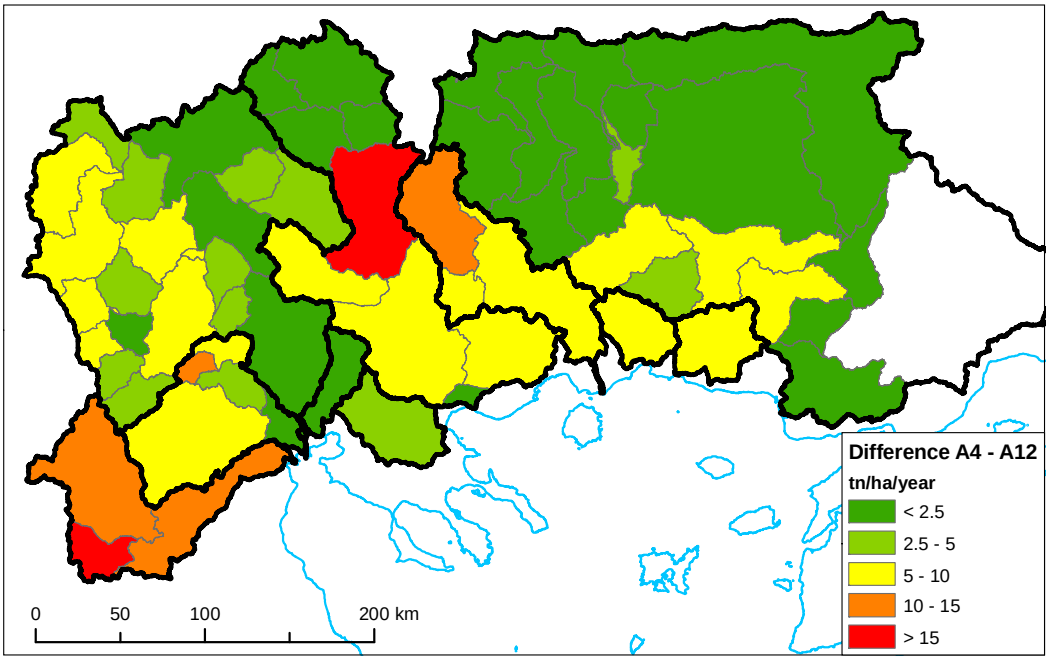

Figure 2: Spatial distribution of the differences between estimating annual soil loss monthly and seasonally.

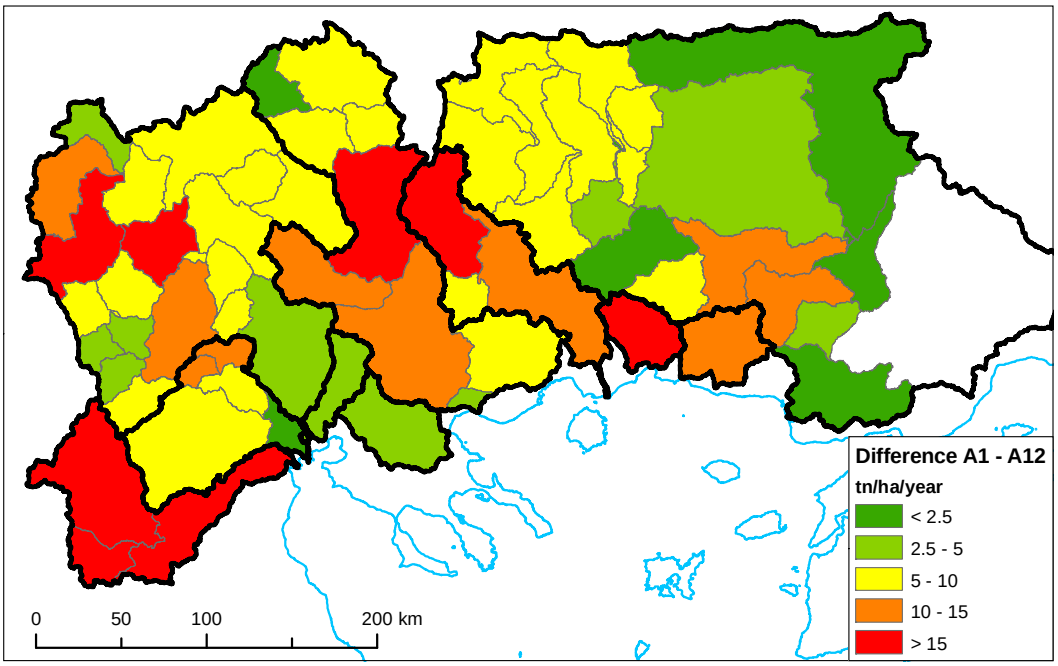

Figure 3: Spatial distribution of the differences between estimating annual soil loss monthly and once in a year.

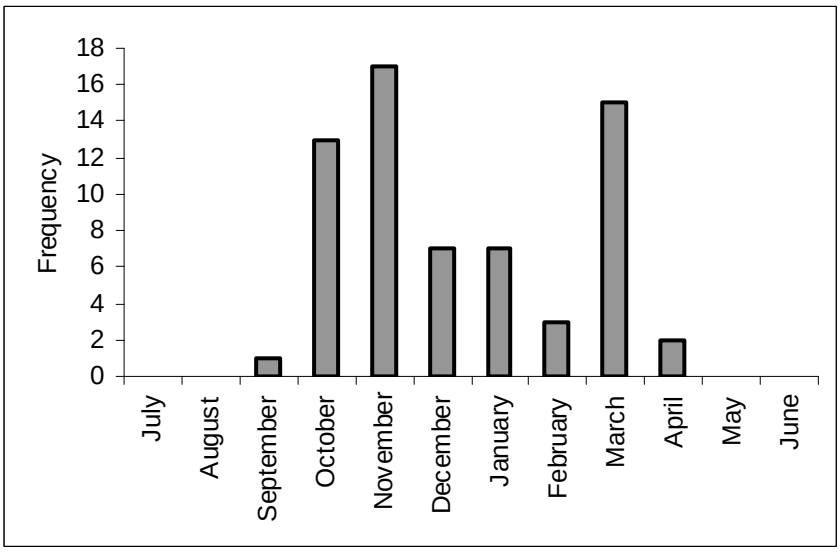

Figure 4: Frequency distribution of optimum single month for estimating annual soil loss, at the subcatchment level.

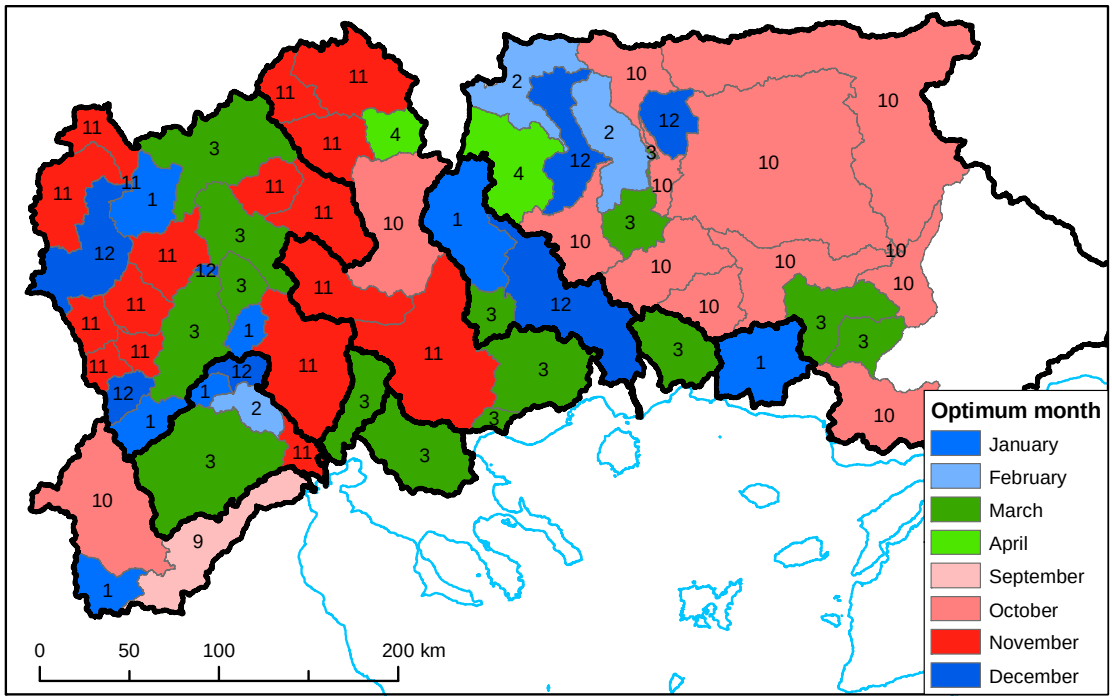

Figure 5: Spatial distribution of the optimum single month for estimating annual soil loss. The label in each subcatchment indicates the optimum month.